Evidence for Long-Lived Quasiparticles Trapped in Superconducting Point Contacts

M. Zgirski, L. Bretheau, Q. Le Masne, H. Pothier,* D. Esteve, and C. Urbina

Quantronics Group, Service de Physique de l'État Condensé (CNRS, URA 2464), IRAMIS, CEA-Saclay, 91191 Gif-sur-Yvette, France

(Received 5 April 2011; published 22 June 2011)

We have observed that the supercurrent across phase-biased, highly transmitting atomic size contacts is strongly reduced within a broad phase interval around π. We attribute this effect to quasiparticle trapping in one of the discrete subgap Andreev bound states formed at the contact. Trapping occurs essentially when the Andreev energy is smaller than half the superconducting gap Δ, a situation in which the lifetime of trapped quasiparticles is found to exceed 100 μs. The origin of this sharp energy threshold is presently not understood.

DOI: 10.1103/PhysRevLett.106.257003 PACS numbers: 74.45.+c, 73.23.−b, 74.50.+r

Both theory and experiment indicate that the number of quasiparticles in superconductors decreases exponentially as the temperature is lowered, while their recombination time increases [1,2]. This slow dynamics is an important ingredient in nonequilibrium superconductivity and allows for the design of high-performance devices like single photon detectors for astrophysical applications [3]. However, recent developments on microwave resonators [4] and Josephson qubits [5] show that at very low temperatures residual nonequilibrium quasiparticles set a limit to the proper functioning of these devices. More drastically, a single quasiparticle can determine the response of single-Cooper-pair devices [6] containing small superconducting islands in which the parity of the total number of electrons actually matters. The trapping of a single quasiparticle in such a superconducting island has been dubbed "poisoning" [7], as it inhibits the behavior expected in the ground state of the system. Remarkably, it has been argued [8] that quasiparticle trapping could also occur in the discrete Andreev bound states [9] formed at subgap energies in a constriction between two superconductors, a system containing no island at all. We demonstrate this phenomenon with an experiment on atomic size constrictions, where the trapping of a single quasiparticle is revealed by the full suppression of the macroscopic supercurrent through its well transmitted conduction channels. We also show that, as anticipated [8], trapped quasiparticles are long-lived, with time scales up to hundreds of μs.

We use microfabricated mechanically controllable break junctions [10] to obtain aluminum atomic point contacts embedded in an on-chip circuit, sketched in Fig. 1(c) [11]. The circuit allows measuring for each atomic contact both the current-voltage characteristic, from which one determines precisely the ensemble $\{\tau_i\}$ of the transmissions of its conduction channels [12], and its current-phase relation [13]. In order to go reversibly from voltage to phase biasing, the atomic contact is placed in parallel with a Josephson tunnel junction (critical current $I_0 \sim 554$ nA much larger than the typical critical current of a one-atom aluminum contact $\sim$50 nA) to form an asymmetric dc SQUID. An on-chip antenna allows applying fast flux pulses through the SQUID loop and a superconducting coil is used to apply a dc flux.

In the usual semiconductor representation, there is just one pair of Andreev bound states in a short one-channel constriction, with energies $\pm E_A(\delta,\tau) = \pm\Delta\sqrt{1-\tau\sin^2(\delta/2)}$ determined by the channel transmission τ and the phase difference δ across it [8,11,14,15]. In the ground state, only the Andreev bound state at negative energy is occupied, leading to a phase dependent term $-E_A(\delta,\tau)$ in the total

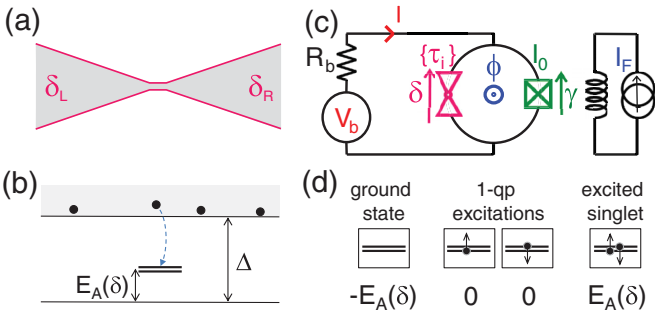

FIG. 1 (color online). (a) Short one-channel constriction between two superconducting electrodes (phase difference $\delta = \delta_L - \delta_R$). (b) Excitation spectrum: besides the usual continuum of states above the energy gap Δ, which extends all across the structure, there is at the constriction a discrete Andreev spin-degenerate doublet with energy $E_A(\delta)$ above the ground state, where quasiparticles can get trapped. (c) Schematic setup: an atomic point contact (red triangles) forms a SQUID with a Josephson junction (green checked box). Phases δ and γ across contact and junction are linked by the flux ϕ threading the loop. The SQUID is biased by a voltage source V_b in series with a resistance $R_b = 200\ \Omega$. The current I is measured from the voltage drop across R_b. An on-chip antenna is used to apply fast flux pulses to the SQUID. It is represented on the right-hand side as an inductor current-biased with a source I_F. (d) Four possible configurations of a one-channel constriction: ground state (energy $-E_A$), Andreev doublet empty; two odd configurations, with zero energy and definite spin $\pm 1/2$, one quasiparticle added to the contact; last configuration corresponds to spin-singlet double excitation (energy $+E_A$).

energy, and a supercurrent $-I_A = -\varphi_0^{-1}\partial E_A/\partial\delta$, with $\varphi_0 = \hbar/2e$. The two Andreev bound states give rise to the excitation spectrum shown in Fig. 1(b), with a discrete spin-degenerate doublet, localized at the constriction, at an energy $E_A \leq \Delta$ above the ground state. The four lowest-lying configurations of the system are built from this doublet. Above the ground state, there are two "odd" configurations (spin 1/2) with a single excitation of the doublet at E_A, i.e., with a quasiparticle trapped in the constriction. In this case the global energy is zero, i.e., phase independent, and the total supercurrent is zero [15]. Finally, there is another spin-singlet configuration with a double excitation, which carries a supercurrent $+I_A$ exactly opposite to the one in the ground configuration. Hence, the supercurrent through the constriction is a probe of the configuration of the system.

In our experiment, the supercurrent through the atomic contact is accessed through measurements of the "switching current" of the SQUID, which is the bias current at which the whole device switches from the supercurrent branch ($V = 0$) to a finite voltage state. Because of the large asymmetry, the SQUID switching current is only slightly modulated around that of the junction by the applied flux ϕ. The modulation corresponds essentially to the current-phase relation of the atomic contact [13]. As the SQUID loop is small, the phase γ across the Josephson junction, the phase δ across the atomic contact, and the phase $\varphi = \phi/\varphi_0$ related to the external flux ϕ are linked [11] through $\varphi = \delta - \gamma$. To measure the switching current of the SQUID, current pulses of variable normalized height $s = I/I_0$ are applied through the bias line, while monitoring the voltage across the SQUID. To ensure that the measurements are statistically independent, additional short prepulses that force switching are applied before each one of them [11] (top left inset of Fig. 2). The switching probability $P_{sw}(s)$ is obtained as the ratio of the number of measured voltage pulses to the number of bias pulses (typically 10^4). In Fig. 2, we show $P_{sw}(s, \varphi)$ measured at 30 mK on one particular SQUID ($\{\tau_i\} = \{0.994, 0.10, 0.10\}$). For most flux values, we observe the generic behavior for Josephson junctions and SQUIDs, i.e., a sharp variation of the probability from 0 to 1 as the pulse height is increased (lower left inset of Fig. 2). However, in a broad flux range $0.7\pi < \varphi < 1.1\pi$ around π, the behavior is completely unusual: $P_{sw}(s)$ increases in two steps and displays an intermediate plateau (top right inset of Fig. 2).

Precise comparison between experiment and theory is performed using an extension [11,13] of the well-known model describing the switching of a Josephson junction as the thermal escape of a particle over a potential barrier [16]. For our SQUIDs, the potential is dominated by the Josephson energy of the junction but contains a small contribution $\sum_i c_i E_A(\gamma + \varphi, \tau_i)$ from the atomic contact, which depends on $\{\tau_i\}$ and on the configuration of its Andreev levels ($c_i = -1$ if channel i is in its ground state, $c_i = 1$ in excited singlet, and $c_i = 0$ in an odd configuration). The predictions for $P_{sw}(s)$ are shown as lines in the insets of Fig. 2. Whereas the data taken at $\varphi = 0$ are well fitted by theory with all channels in the ground state, those taken at $\varphi = 0.88\pi$ are not. However, they can be very precisely accounted for by the weighted sum of the theoretical curves $P^0_{sw}(s)$ and $P^1_{sw}(s)$ corresponding, respectively, to the "pristine contact" (i.e., with all channels in their ground configuration), and to the "poisoned" contact (i.e., with its most transmitted channel in an odd configuration). This is the case in the whole flux region where the measured switching curves have an intermediate plateau, showing that

$$P_{sw}(s, \varphi) = [1 - p(\varphi)]P^0_{sw}(s, \varphi) + p(\varphi)P^1_{sw}(s, \varphi). \quad (1)$$

The function $1 - p(\varphi)$ describes the height of the intermediate plateau in $P_{sw}(s)$. A similar analysis was performed for other SQUIDs formed with atomic contacts having one highly transmitted channel [11], and in all cases, $P_{sw}(s)$ shows a plateau delimited by the predictions for the pristine and the poisoned contact in a broad phase

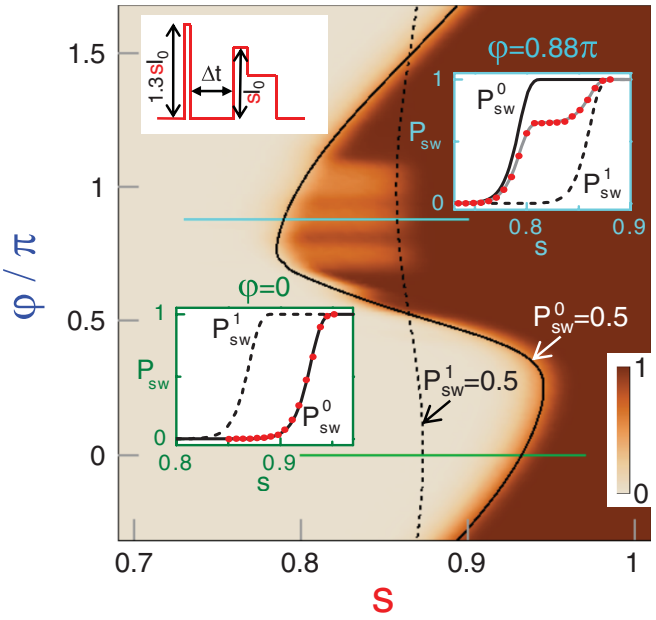

FIG. 2 (color online). Color plot of measured switching probability $P_{sw}(s, \varphi)$ for SQUID with contact transmissions {0.994, 0.10, 0.10}. Top left inset: Measurement protocol. Short prepulses ensure the same initial conditions before each measurement pulse of height $I = sI_0$ and duration $t_p = 1$ μs (the subsequent lower plateau holds the voltage to facilitate detection). Delay between prepulse and measurement pulse is here $\Delta t = 2$ μs. Main panel: Black curves represent theoretical predictions [solutions of $P_{sw}(s, \varphi) \equiv 0.5$] for pristine (solid line) and for poisoned contact (dashed line). Lower left inset: Measured $P_{sw}(s)$ (red dots) at $\varphi = 0$ [lower horizontal (green) line in main panel]. Upper right inset: Measured $P_{sw}(s)$ (red dots) at $\varphi = 0.88\pi$ [upper horizontal (cyan) line in main panel]. In both insets $P^0_{sw}(s)[P^1_{sw}(s)]$, the solid [dashed] line is the theory for the pristine [poisoned] contact. In the upper right inset, the intermediate line (gray solid line) is a fit of the data with the linear combination of Eq. (1) with $p = 0.36$.

range around π. The fact that the data are precisely accounted for by this linear combination induces us to interpret the coefficient p as the poisoning probability, i.e., the probability for the atomic contact to have a quasiparticle trapped in its most transmitting channel.

We have found that at fixed s and φ, the poisoning probability p depends exponentially on the delay Δt between the prepulse and the measurement pulse (Fig. 3 right inset): a fit of the form $p(\Delta t) = p_\infty + (p_0 - p_\infty)\times \exp(-\Delta t/T_1)$ gives the initial poisoning just after the prepulse p_0, the asymptotic value at long times p_∞, and the relaxation time T_1. To obtain a meaningful measurement of the phase dependence of the relaxation, we had to implement a refined protocol [11] involving flux pulses applied through the fast flux line within the time interval Δt. It allows probing the relaxation from a fixed p_0, with measurement occurring always at the same flux, the only adjustable parameter being the phase δ during the waiting time. Both $p_\infty(\delta)$ and $T_1(\delta)$, measured at 30 mK, are shown in Fig. 3 for the same SQUID as in Fig. 2. Their phase dependence is symmetric and peaked at $\delta = \pi$, where the relaxation is the slowest and p_∞ the largest. A rapid decay of T_1 by almost 2 orders of magnitude and a drop of p_∞ to 0 are observed at $|\delta - \pi| \simeq 0.3\pi$. The overall shape of both $p_\infty(\delta)$ and $T_1(\delta)$ remains very similar when temperature is varied [11]. The relaxation time T_1 falls rapidly with temperature, and becomes too short to be measured above 250 mK. Similar data [11] taken on a variety of atomic contacts show that the phase interval in which poisoning occurs reduces when the transmission of the most transmitting channel diminishes. For channels with all transmissions smaller than 0.7, the poisoning probability p was too small to be measured. An important observation is that when two switching prepulses are applied (instead of a single one) with more than 1 μs delay between them, the first one has no effect, which indicates

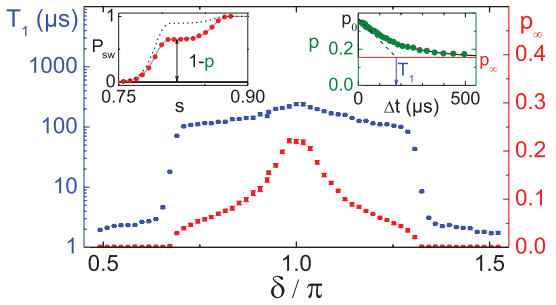

FIG. 3 (color online). Relaxation time T_1 (blue points) and asymptotic poisoning probability p_∞ (red points) as a function of the phase δ imposed for a time Δt between prepulse and measurement pulse. Data taken on SQUID with atomic contact {0.994,0.10,0.10} at 30 mK. Measurements at $|\delta - \pi| > 0.5\pi$ show very fast relaxation that could not be resolved reliably in our setup. Left inset: 1-p is the height of the intermediate plateau in $P_{sw}(s)$. The dashed line represents $P_{sw}(s)$ found for $\Delta t \gg 100$ μs. Right inset: Typical time evolution of p, from where T_1 and p_∞ are extracted.

that quasiparticles created by switching matter only during 1 μs. This experimental observation, plus the fact that diffusion is expected to efficiently drain away from the constriction the quasiparticles created by the prepulse [11], allow us to conclude that the residual quasiparticle density is constant during the poisoning probability relaxation, and that it does not originate from the switching pulses (contrary to p_0). The fact that $p_\infty \neq 0$ proves that quasiparticles are present in the continuum in the steady state, as found in other experiments [4,17,18].

When quasiparticles jump between the Andreev states and the states in the continuum, transitions arise among the four configurations accessible to the Andreev doublet, as shown in the inset of Fig. 4. All the microscopic processes involved are in principle rather slow because they require either energy absorption or the presence of quasiparticles in the continuum [8]. We define the rates Γ_{in} and Γ_{out}

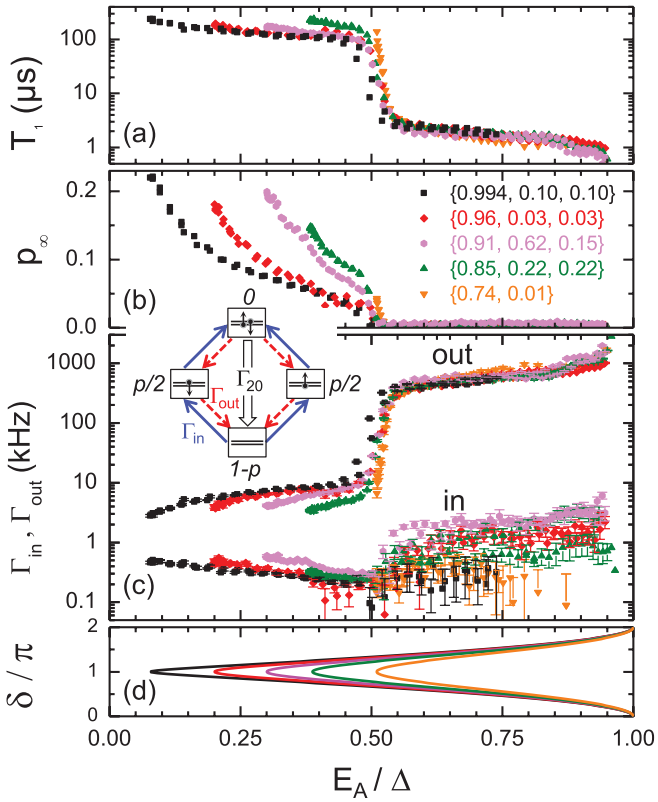

FIG. 4 (color online). Relaxation data for five different atomic contacts [transmissions are given in panel (b)]: (a) relaxation time T_1, (b) asymptotic poisoning probability p_∞, (c) rates Γ_{in} and Γ_{out} as a function of normalized Andreev state energy E_A/Δ of most transmitting channel. There is a sharp threshold at $E_A/\Delta \approx 0.5$ for all contacts. The minimal value of E_A/Δ is $\sqrt{1-\tau}$ (0.08 for the black squares, 0.5 for the orange upside-down triangles) and is reached when $\delta = \pi$, as shown in (d). Inset: Rates Γ_{in} (Γ_{out}) are for processes increasing (decreasing) the number of quasiparticles in contact. The relaxation rate from the excited singlet to the ground state is assumed to be much faster than all other rates. The occupation of all four configurations is given in italic letters: 1-p for the ground state, $p/2$ for each of the odd configurations, and 0 for the excited state.

corresponding to an increase or a decrease of the number of quasiparticles in the contact. Because we see no trace of the state with a double excitation either in these data or in preliminary spectroscopic measurements, we assume that the relaxation rate Γ_{20} to the ground state is much larger than Γ_{in} and Γ_{out}. From a simple master equation [11] for the population $1-p$ of the ground state, and $p/2$ of each of the odd configurations, one gets

$$T_1 = \frac{1}{\Gamma_{out} + 3\Gamma_{in}}, \qquad p_\infty = \frac{2\Gamma_{in}}{\Gamma_{out} + 3\Gamma_{in}}, \tag{2}$$

and the flux dependence of Γ_{in} and Γ_{out} can then be extracted from the data. Then, instead of plotting the results as a function of the applied flux δ like in Fig. 3, we choose for the x axis the Andreev energy $E_A(\delta)$ of the most transmitting channel. The results for five contacts are shown in Fig. 4, together with the relaxation time T_1 and asymptotic poisoning probability p_∞. Although the Andreev energy is clearly not the only relevant parameter, the rates for all contacts roughly coincide. The most apparent differences are in the asymptotic poisoning probability p_∞ which, for a given E_A, diminishes when the transmission of the most transmitting channel increases. Two distinct regimes are evidenced in Fig. 4: When $E_A/\Delta > 0.5$, the relaxation time is very short and the asymptotic poisoning is negligible. In terms of rates, Γ_{in} is smaller than Γ_{out} by 2 to 3 orders of magnitude. In contrast, when the Andreev energy lies deep in the gap ($E_A/\Delta < 0.5$), relaxation is much slower and the asymptotic poisoning probability becomes sizable. This regime corresponds to a smaller ratio Γ_{out}/Γ_{in}. The sharp threshold at $E_A/\Delta \simeq 0.5$, where Γ_{out} drops by 2 orders of magnitude, is observed for all the measured contacts with highest transmission above 0.74. Furthermore, no poisoning was observed in contacts in which all channels had transmissions below 0.74, the Andreev state energy then being always larger than $\Delta\sqrt{1-0.74} \sim 0.5\Delta$. In contrast, we have found that in contacts with more than one highly transmitting channel, poisoning can affect several channels at once [11]. Presently, we do not have an explanation for the energy dependence of the rates: the mechanisms commonly used to describe quasiparticle dynamics in superconductors (recombination, phonon emission, and absorption) do not lead to such a sharp threshold at energy 0.5Δ.

Let us mention that it is possible to untrap quasiparticles. For example, we have implemented an efficient ''antidote'' protocol [11] based on dc flux pulses that bring the Andreev states at the gap edge from where the trapped quasiparticle can diffuse away into the electrodes. Furthermore, it is possible to avoid poisoning altogether: when the large scale on-chip wires connecting to the SQUID are made out of either a normal metal [13] or a superconductor with a lower gap than the device [11], they act as good quasiparticle traps and poisoning is never observed.

To conclude, we have performed the first observation and characterization of single quasiparticles trapped in Andreev bound states. The long lifetimes that we have measured open the way to individual spin manipulation and to superconducting spin qubits [8]. Moreover the complete suppression of the macroscopic supercurrent when a single quasiparticle is trapped shows that a superconducting quantum point contact can be seen as a very efficient quasiparticle detector. Finally, let us mention that quasiparticle trapping, which is likely to be a generic phenomenon in superconducting weak links, could be detrimental in some situations. It could be the case for experiments proposed to detect ''Majorana bound states'' in condensed matter systems [19] since their topological protection relies on parity conservation.

We thank H. Grabert, A. Levy Yeyati, J. Martinis, V. Shumeiko, and D. Urban for enlightening discussions. We gratefully acknowledge help from other members of the Quantronics group, in particular, P. Senat and P. F. Orfila for invaluable technical assistance. Work was partially funded by ANR through projects CHENANOM, DOCFLUC, and MASQUELSPEC, and by C'Nano IdF.

*Corresponding author.
hugues.pothier@cea.fr

[1] S. B. Kaplan *et al.*, Phys. Rev. B **14**, 4854 (1976).
[2] C. M. Wilson, L. Frunzio, and D. E. Prober, Phys. Rev. Lett. **87**, 067004 (2001).
[3] P. K. Day *et al.*, Nature (London) **425**, 817 (2003).
[4] P. J. de Visser *et al.*, Phys. Rev. Lett. **106**, 167004 (2011).
[5] M. Lenander *et al.*, arXiv:1101.0862v1 [Phys. Rev. B (to be published)].
[6] P. Joyez *et al.*, Phys. Rev. Lett. **72**, 2458 (1994).
[7] J. Aumentado *et al.*, Phys. Rev. Lett. **92**, 066802 (2004).
[8] N. M. Chtchelkatchev and Yu. V. Nazarov, Phys. Rev. Lett. **90**, 226806 (2003).
[9] A. Furusaki and M. Tsukada, Solid State Commun. **78**, 299 (1991); C. W. J. Beenakker and H. van Houten, Phys. Rev. Lett. **66**, 3056 (1991).
[10] J. van Ruitenbeek *et al.*, Rev. Sci. Instrum. **67**, 108 (1996).
[11] See supplemental material at http://link.aps.org/supplemental/10.1103/PhysRevLett.106.257003 for additional data and details on sample fabrication, measurement techniques, and modeling.
[12] E. Scheer *et al.*, Phys. Rev. Lett. **78**, 3535 (1997).
[13] M. L. Della Rocca *et al.*, Phys. Rev. Lett. **99**, 127005 (2007).
[14] J. Michelsen, V. S. Shumeiko, and G. Wendin, Phys. Rev. B **77**, 184506 (2008).
[15] In a spin-degenerate system.
[16] P. Hänggi, P. Talkner, and M. Borkovec, Rev. Mod. Phys. **62**, 251 (1990).
[17] M. D. Shaw *et al.* , Phys. Rev. B **78**, 024503 (2008).
[18] John M. Martinis, M. Ansmann, and J. Aumentado, Phys. Rev. Lett. **103**, 097002 (2009).
[19] L. Fu and C. L. Kane, Phys. Rev. Lett. **100**, 096407 (2008).